Journal of Alloys and Compounds 503 (2010) 86–91

Contents lists available at ScienceDirect

Journal of Alloys and Compounds

journal homepage: www.elsevier.com/locate/jallcom

Influence of X-ray irradiation on the optical properties of ruthenium(II)octa-(*n*-hexyl)-phthalocyanine thin film

M.M. El-Nahass[a,*], Tamer E. Youssef[b]

[a] *Physics Department, Faculty of Education, Ain Shams University, Roxy Square 11757, Cairo, Egypt*
[b] *Applied Organic Chemistry Department, National Research Center, Dokki, 12311, Cairo, Egypt*

ARTICLE INFO

Article history:
Received 8 January 2010
Received in revised form 27 March 2010
Accepted 1 April 2010
Available online 13 April 2010

Keywords:
Phthalocyanines
Ruthenium thin films
Optical properties

ABSTRACT

Ruthenium(II)octa-(*n*-hexyl)-phthalocyanine [(*n*-hexyl)$_8$PcRu] (**2**) thin films have been deposited on different substrates by thermal evaporation technique under high vacuum. X-ray diffraction (XRD) pattern of [(*n*-hexyl)$_8$PcRu] (**2**) in the powder form indicated that it has polycrystalline form with a triclinic structure. The XRD results for [(*n*-hexyl)$_8$PcRu] (**2**) thin films confirm the amorphous nature for the as-deposited films. The optical properties of [(*n*-hexyl)$_8$PcRu] (**2**) were investigated for as-deposited and irradiated films using spectrophotometric measurements of the transmittance and reflectance at normal incidence of light in the wavelength range from 200 to 2500 nm. The recorded absorption measurements in the UV–vis region show two well defined absorption bands of phthalocyanine molecule; namely the Q-band and the Soret (B-band). The refractive index (n) and the absorption index (k) were calculated. According to the analysis of dispersion curves, the parameters, namely; the optical absorption coefficient (α), molar extinction coefficient (ε_{molar}), oscillator energy (E_o), oscillator strength (f), and electric dipole strength (q^2) were also evaluated. The analysis of the spectral behaviour of the absorption coefficient (α), in the absorption region revealed indirect transitions.

1. Introduction

Continuing attention has been paid to the systematic study to understand the physical properties of organic complex solids owing to the enhanced mechanical, thermal, magnetic, optical, electronic, and optoelectronic properties. This leads to increase the possibility of implementing innovative applications in many adjacent disciplines such as nanotechnology, sensors and photonics [1–3]. Among the wide range of organic semiconductors considered, metal phthalocyanines (Pcs) with excellent growth properties with chemical and thermal stability, are one of the most promising candidates for the production of the majority of modern optoelectronic devices [4]. These have been exploited in modern optoelectronic devices such as photoconductors [5] and also as active components in organic electronic devices [6] like organic light-emitting diodes [7], organic field effect transistors [8,9] and organic photovoltaic cells [3]. Extensive work has been carried out on numerous metal phthalocyanines [2,10], ruthenium phthalocayanine (RuPc), which tends to be a promising compound due to its chemical–physical behaviour, it remains largely unexplored in these areas [11].

Our present research work, some of the structural and optical properties of thermally evaporated ruthenium phthalocayanine (RuPc) thin films were investigated. Complex (**2**) was prepared by modifying the synthetic method carried out by Hanack et al. [12,13]. They have prepared ruthenium phthalocyanine complexes with no peripheral substituent. Our research group has synthesized a series of octaalkoxy-substituted phthalocyanine complexes with identical peripheral substituents in the 2, 3, 9, 10, 16, 17, 23, 24 positions [14,15]. Really, we cannot determine the exact structure of the obtained [(*n*-hexyl)$_8$PcRu] (**2**) it could be as an amorphous or microcrystalline material. PcRu has been examined by large-angle X-ray scattering (LAXS) by Ercolani et al. [16] and they deduced a dimeric structure (PcRu)$_2$ with a short Ru–Ru contact of 2.40 Å from the obtained data. This agree with the values appeared in the Fast Atom Bombardment (FAB) mass spectrum m/z 2573.78 (M^+)$_2$, 1286.89 (M^+), which indicates that the presence of **2** in a dimeric structure [(*n*-hexyl)$_8$PcRu]$_2$.

IR spectroscopy has been used in comparison with [(PcRu)$_2$] as a bulk solid and in thin film and it shows differences in the out of plane C–H bending region (800–700 cm^{-1}). This and the absence of a peak at 866 cm^{-1} in the thin film specimen were attributed to different molecular assemblies [17].

2. Experimental procedures

2.1. Materials

The starting materials for the syntheses were purchased from Lancaster and Aldrich, and used as received. Precursor 4,5-di-*n*-hexylphthalonitrile (**1**) was

* Corresponding author.
E-mail address: prof_nahhas@yahoo.com (M.M. El-Nahass).

0925-8388/$ – see front matter © 2010 Elsevier B.V. All rights reserved.
doi:10.1016/j.jallcom.2010.04.029

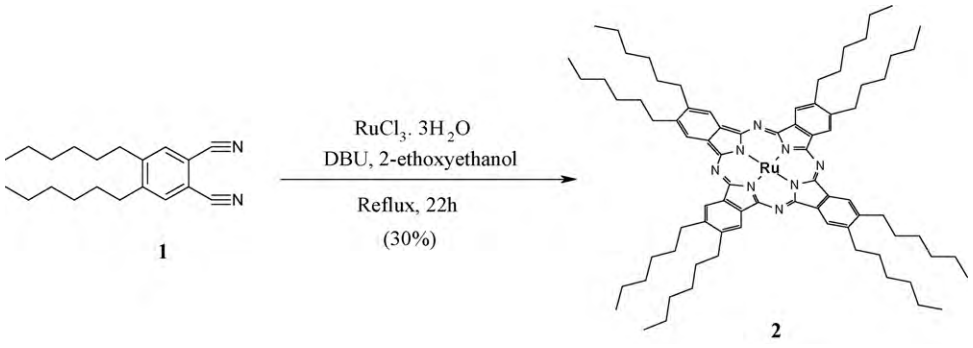

Fig. 1. Synthesis of 2,3,9,10,16,17,23,24-octa(*n*-hexyl)phthalocyaninatoruthenium(II) (**2**).

synthesized as described in another report to prepare the octasubstituted phthalocyaninatoplatinum and palladium complexes [18]. The scheme of reaction to obtain [(*n*-hexyl)$_8$PcRu] (**2**) is shown in Fig. 1.

2.2. Synthesis of 2,3,9,10,16,17,23,24-octa(n-hexyl)phthalocyaninatoruthenium(II) (2)

A mixture of 4,5-di-*n*-hexylphthalonitrile (1.2 g, 3.64 mmol), ruthenium(III) chloride trihydrate (0.26 g, 1 mmol) and diazabicyclo[5.4.0]undec-7-ene (DBU) (0.45 g, 3 mmol) was stirred in 2-ethoxyethanol (10 ml) under nitrogen at reflux temperature for 22 h. The reaction mixture was then cooled to room temperature, methanol (7 ml) and water (10 ml) was added, and the mixture was stirred at room temperature for 4 h. The precipitated solid was filtered off, washed with a methanol/water mixture (1/1, v/v) and dried under vacuum. The crude product (0.48 g) was subjected to column chromatography (50 g of silica gel, chloroform eluent) to yield 0.37 g (30%) of compound **2** as blue violet powder. ^{1}H NMR ($CDCl_3$) 0.9–1.04 (t, 24H, J = 7.2 Hz, 8× CH_3), 1.3–1.8 (m, 48H, 4× $(CH2)_6$), 1.9 (m, 16H, 8× $ArCH_2$ CH_2), 3.2 (t, 16H, J = 6.4 Hz, 8× $ArCH_2$), 8.54 (s, 8H, Ar–H). UV–vis ($CHCl_3$), λ_{max} (nm): 628, 376, 325. MS (FAB): m/z 2573.78 $(M^+)_2$, 1286.89 (M^+). Elemental analysis: found C 74.67, H 8.77, N 8.71 (Calcd. C 73.82, H 8.20, N 8.56).

2.3. Film deposition and measurements

The films were deposited onto different substrates, glass substrates for X-ray diffraction (XRD) analysis and optical flat quartz substrates for the optical measurements. Thin films of [(*n*-hexyl)$_8$PcRu] (**2**) were prepared by conventional thermal evaporation technique, using a high vacuum coating unit (Edwards type E306 A, England). [(*n*-Hexyl)$_8$PcRu] (**2**) was sublimed from a quartz crucible heated by a tungsten coil in a vacuum of 10^{-4} Pa. The deposition rate was controlled at 2.5 nm s^{-1} by using a quartz crystal thickness monitor (Model FTM4, Edward Co., England). Film thickness was monitored by the same thickness monitor and subsequently calibrated by Tolansky method [19].

The structural investigation of [(*n*-hexyl)$_8$PcRu] (**2**) in the powder and thin film forms was analyzed by XRD technique. Philips X-ray diffractometer (model X′ Pert) was used for this measurement. The transmittance $T(\lambda)$ and the reflectance $R(\lambda)$ spectra for [(*n*-hexyl)$_8$PcRu] (**2**) films were measured at normal incidence in the spectral range 200–2500 nm using a double beam spectrophotometer (JASCO model V-570 UV–vis–NIR). The films were exposed to high-energy X-ray (6 MeV); the dose of irradiation was 20 kGy by using a linear accelerator (Philips electronics UK version SL15).

The absolute values of T and R at different wavelengths (making base line correction with the substrates) are given by the following equation [20,21]:

$$T = \left(\frac{I_{ft}}{I_q}\right)(1 - R_q) \quad (1)$$

where I_{ft} and I_q are the intensities of light passing through the film-quartz system and that through the reference-quartz, respectively. R_q is the reflectance of quartz substrate, and

$$R = \left(\frac{I_{fr}}{I_m}\right) R_m \left[(1 + (1 - R_q)^2)\right] - T^2 R_q \quad (2)$$

where I_{fr} is the intensity of light reflected from the sample reaching the detector, I_m is the intensity of light reflected from the reference mirror and R_m is the mirror reflectance

In order to calculate the optical constants, refractive index, n, and the absorption index, k, of the films at different wavelengths, we can use the following equations [22]:

$$\alpha = \frac{1}{d} \ln\left[\frac{(1-R)^2}{2T} + \sqrt{\frac{(1-R)^4}{4T^2} + R^2}\right] \quad (3)$$

$$n = \frac{1+R}{1-R} + \sqrt{\frac{4R}{(1-R)^2} - k^2} \quad (4)$$

$$k = \frac{\alpha\lambda}{4\pi} \quad (5)$$

where α is the absorption coefficient. When the thickness of film (d) is known, then the computation can be carried out and the optical constant can be calculated. The experimental error in measuring the film thickness was taken as ±2%, in T and R as ±1% and in the calculated values of n and k was estimated to be 3% and 2.5%, respectively.

3. Results and discussion

3.1. Structural investigations

Fig. 2a shows the XRD pattern of [(*n*-hexyl)$_8$PcRu] (**2**) in the powder form taken in a 2θ range from 2° to 50°. The pattern has many peaks with different intensities; this result indicates that the material under investigation is in polycrystalline form. The unit cell parameters of [(*n*-hexyl)$_8$PcRu] (**2**) were determined by using the CRYSFIRE computer program [23]. The values of Miller indices, $h\,k\,l$, and lattice spacing, d_{hkl}, corresponding to each diffraction line was indexed using CHECKCELL program [24] and the results are given in Table 1. The analysis indicates that [(*n*-hexyl)$_8$PcRu] (**2**) has triclinic structure with space group $P\bar{1}$. Lattice parameters cell are a = 9.882 Å, b = 12.448 Å, c = 19.761 Å, α = 108.81°, β = 87.94° and γ = 84.29°. Fig. 2(b) and (c) shows the XRD pattern of as-deposited and irradiated films onto glass substrates. The absence of sharp diffraction peaks and the presence of humps emphasize amorphous nature.

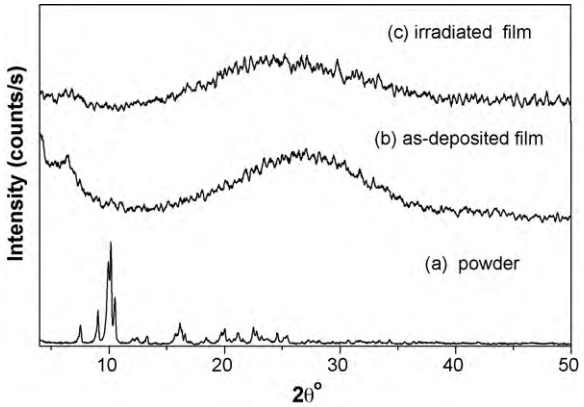

Fig. 2. X-ray pattern of [(*n*-hexyl)$_8$PcRu] (**2**) (a) the powder form, (b) as-deposited, and (c) irradiated thin films.

Table 1
X-ray indexing for the powder of [(n-hexyl)$_8$PcRu] (**2**).

No.	2θ measured	2θ calculated	d measured	d calculated	I/I_o	hkl	No.	2θ measured	2θ calculated	d measured	d calculated	I/I_o	hkl
1	7.5477	7.549	11.703	11.702	16.03	0 1 0	18	20.0383	20.066	4.4274	4.421	14.59	0 $\bar{2}$ 4
2	9.0522	9.009	9.7611	9.808	32.75	1 0 0	19	20.3930	20.383	4.3512	4.353	4.99	$\bar{1}$ $\bar{1}$ 4
3	9.9153	9.873	8.9132	8.952	78.26	1 0 1	20	20.8148	20.873	4.2610	4.252	4.68	2 $\bar{1}$ 2
4	10.1776	10.147	8.6841	8.711	100	0 1 1	21	21.2045	21.21	4.1865	4.189	11.08	$\bar{1}$ 1 3
5	10.5216	10.48	8.4009	8.434	46.33	$\bar{1}$ 0 1	22	21.5998	21.592	4.1107	4.112	5.37	2 1 2
6	12.0259	12.134	7.3532	7.288	5.22	1 $\bar{1}$ 1	23	22.4957	22.494	3.9490	3.949	16.20	0 $\bar{1}$ 5
7	12.4415	12.428	7.1086	7.17	5.36	1 $\bar{1}$ 0	24	22.7830	22.78	3.8999	3.901	12.51	0 3 0
8	13.326	13.334	6.3877	6.638	7.03	$\bar{1}$ $\bar{1}$ 2	25	23.2111	23.311	3.8289	3.813	8.07	$\bar{1}$ 2 2
9	13.976	13.936	6.3313	6.35	0.63	0 1 2	26	23.7096	23.719	3.7495	3.748	5.09	$\bar{1}$ $\bar{3}$ 3
10	15.722	15.734	5.6320	5.628	8.12	$\bar{1}$ $\bar{1}$ 2	27	24.5699	24.588	3.6201	3.618	10.00	$\bar{1}$ $\bar{1}$ 5
11	16.137	16.129	5.4879	5.491	20.71	1 2 1	28	25.1442	25.074	3.5387	3.522	5.95	2 $\bar{1}$ 4
12	16.337	16.303	5.4214	5.433	12.85	1 0 3	29	25.453	25.414	3.509	3.508	7.18	1 $\bar{2}$ 5
13	16.584	13.54	5.3410	5.355	10.17	$\bar{1}$ $\bar{1}$ 3	30	27.2917	27.301	3.2650	3.264	3.87	0 $\bar{1}$ 5
14	17.088	17.053	5.1846	5.195	1.45	0 $\bar{2}$ 3	31	27.6967	27.69	3.2181	3.217	3.09	0 $\bar{2}$ 6
15	17.989	18.003	4.9270	4.923	2.06	0 $\bar{1}$ 4	32	28.1967	28.242	3.1622	3.157	3.33	3 0 2
16	18.410	18.356	4.8150	4.829	6.04	2 0 1	33	29.3560	29.345	3.0399	3.041	1.75	$\bar{1}$ $\bar{4}$ 2
17	19.7082	19.669	4.5008	4.51	11.40	1 $\bar{2}$ 3							

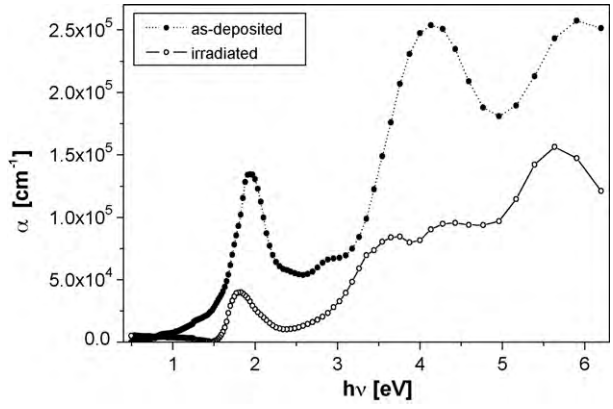

Fig. 3. The spectral distribution of the absorption coefficient (α) of as-deposited and irradiated [(n-hexyl)$_8$PcRu] (**2**) thin films.

3.2. Optical characterization

3.2.1. UV–vis absorption spectra

The absorption coefficient spectrum (α) of [(n-hexyl)$_8$PcRu] (**2**) thin film is shown in Fig. 3. The UV–vis spectrum observed for phthalocyanines originates from molecular orbital within the aromatic π-electron system and from overlapping orbital on the central metal atom [25,26]. The absorption coefficient (α) can be calculated from the absorption index (k) using the formula ($\alpha = 4\pi k/\lambda$). Close examination of the absorption band in the visible region, known as Q-band. The Q-band consists of one peak at 1.94 eV which have been assigned to π–π* transitions on the phthalocyanine macrocycle and one shoulder at 2.76 while for irradiated films 1.82 and 3.76 eV. In the UV spectral region there is an intense band called Soret (B-band) at 4.13 eV and 4.59 eV for as-deposited and irradiated films. The C-band is another region of absorption peaks at 5.9 eV and 5.64 eV.

Table 2 represents the corresponding energies of the orbital transitions (in eV) which are seen in the absorption coefficient spectra of the as-deposited [(n-hexyl)$_8$PcRu] (**2**) and irradiated thin films.

It is useful to relate the absorption coefficient (α) to the molar extinction coefficient (ε_{molar}), which is often used to describe the absorption of light by nonsolid molecular media [27]. If the solid has a concentration of N molecules per unit volume, with molecular weight M, then the absorption coefficient (α) can be expressed in the form

$$\alpha = 2303 \left(\frac{\rho}{M}\right) \varepsilon_{molar} \quad (6)$$

where ρ is the solid's mass density, and (ε_{molar}) is in units of (liters per mole cm)$^{-1}$.

The spectral distribution of the molar extinction coefficient of [(n-hexyl)$_8$PcRu] (**2**) and irradiated thin films is shown in Fig. 4(a) and (b). The spectral parameters, namely oscillator strength (f), electric dipole strength q^2, are determined from the following expressions [27]:

$$f = 4.38 \times 10^{-9} \int \varepsilon_{molar} d\nu \quad (7)$$

$$q^2 = \frac{1}{2500} \varepsilon_{molar} \frac{\Delta\lambda}{\lambda} \quad (8)$$

By using the Gaussian fit, the spectral parameters have been calculated and given in Table 2. The obtained results are in reasonable agreement with previously reported results of other metal phthalocyanines [26–29].

3.2.2. The optical properties

The spectral behaviour of transmittance (T) and the reflectance (R), in the wavelength range 200–2500 nm for as-deposited [(n-hexyl)$_8$PcRu] (**2**) and irradiated thin film of thickness 143 nm is presented in Fig. 5 as a representative sample. The spectra can be

Table 2
Calculated spectral parameters of [(n-hexyl)$_8$PcRu] (**2**) thin film at different bands.

Peak energy (eV)		f		q^2 (Å)^2	
As-deposited film	Irradiated film	As-deposited film	Irradiated film	As-deposited film	Irradiated film
1.94	1.82	0.47	0.10	2.19	0.48
2.76	–	0.20	–	0.65	–
–	3.76	–	0.73	–	1.74
4.13	–	1.88	–	4.18	–
–	4.59	–	0.10	–	0.20
5.90	5.64	3.22	1.53	4.87	2.42

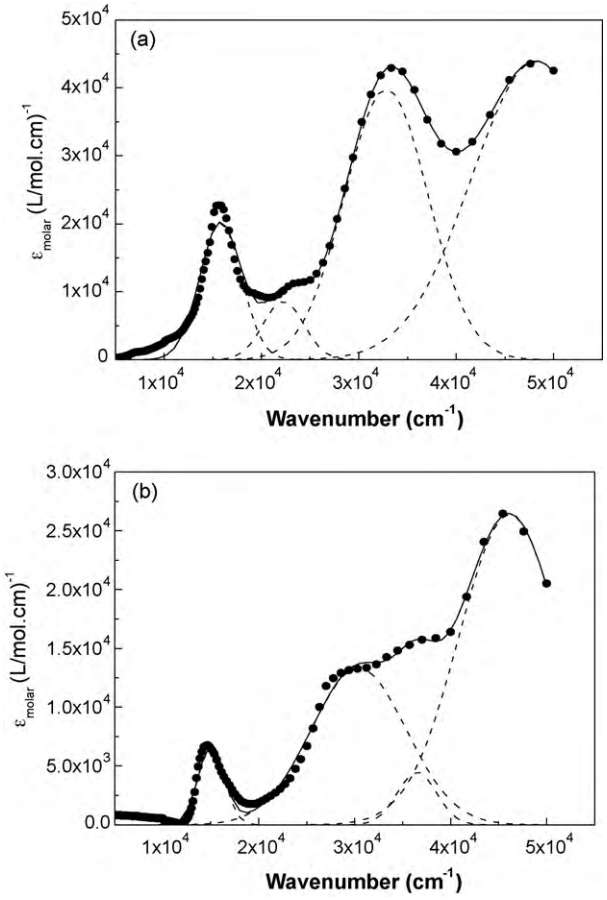

Fig. 4. Molar extinction coefficient versus wave number (circle points) for (a) as-deposited, (b) irradiated thin films of [(*n*-hexyl)$_8$PcRu] (**2**) fitted using the Gaussian model (solid line) assuming five oscillator components. The dashed lines present the decomposition of the molar extinction spectrum on particular oscillatory transitions.

divided into two regions: (a) in the wavelength range from 200 nm to 900 nm, the total sum of $T(\lambda)$ and $R(\lambda)$ is less than unity (absorption region), (b) at longer wavelength 900 nm, $T+R=1$, the film becomes transparent and no light was scattered or absorbed.

The values of transmittance and reflectance were used to determine the optical refractive index, n, and extinction coefficient, k, and absorption coefficient, α; using a special computer program [30].

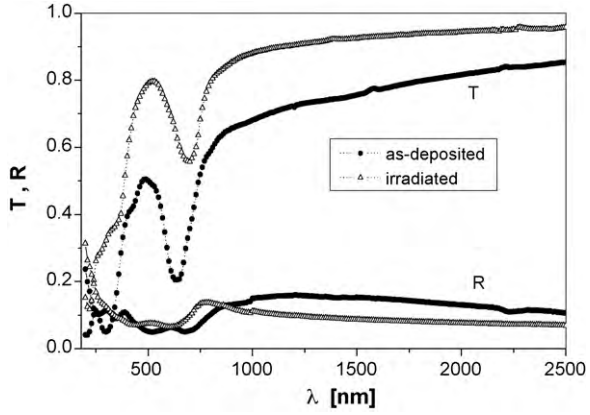

Fig. 5. The spectral distribution of transmittance $T(\lambda)$ and reflectance $R(\lambda)$ for as-deposited and irradiated [(*n*-hexyl)$_8$PcRu] (**2**) thin films.

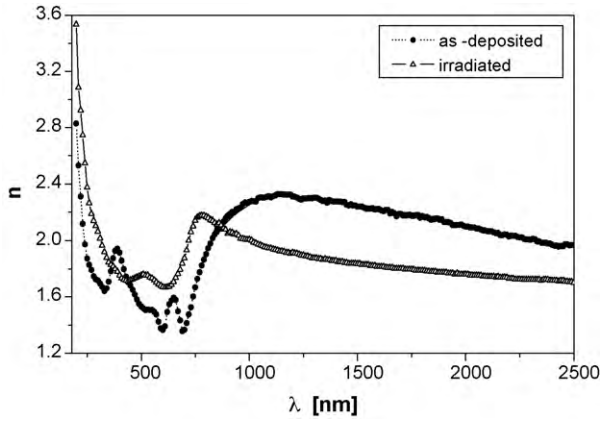

Fig. 6. The dispersion curve of refractive index $n(\lambda)$ for as-deposited and irradiated [(*n*-hexyl)$_8$PcRu] (**2**) thin films.

The dispersion curves of the refractive index, n, in the wavelengths range 200–2500 nm for the as-deposited and irradiated films are presented in Fig. 6. The anomalous dispersion in the wavelength range 200–900 nm, in showing three peaks, while a normal dispersion is observed in the range 900–2500 nm. The dispersion data of the refractive index were analyzed by using the single oscillator model developed by Wemple and DiDomenico [31], who found that the refractive index in the transparent region can be described, to a very good approximation, by the following formula:

$$(n^2-1)^{-1}=\frac{E_o^2-(h\nu)^2}{E_dE_o} \tag{9}$$

where $h\nu$ is the photon energy, E_o is the oscillator energy and E_d is the dispersion energy. Fig. 7a shows the relation between $(n^2-1)^{-1}$ and $(h\nu)^2$ for the as-deposited and irradiated thin films. The values of E_o and E_d are directly determined from the slope and the intercept of the extrapolation to the vertical axis respectively. The calculated values of the dispersion parameters E_o and E_d as well as the corresponding dielectric constant at infinite frequencies ($\varepsilon_\infty=n_\infty^2$) for the as-deposited films were found to be 2.835 eV, 4.805 eV and 4.77 eV for as-deposited and for irradiated films 2.11 eV, 4.213 eV, and 3.0 eV respectively.

The obtained data of refractive index (n) can be analyzed to obtain the high frequency dielectric constant via a procedure describes the contribution of the free carriers and the lattice vibration modes of the dispersion.

The relation between the lattice dielectric constant, ε_L, wavelength, λ, and the refractive index, n, is given by the relation [27]

$$\varepsilon_1=n^2=\varepsilon_L-\frac{e^2N}{4\pi^2\varepsilon_o m*c^2}\lambda^2 \tag{10}$$

where ε_L is the lattice dielectric constant, e is the elementary charge and N/m* is the ratio of carrier concentration, N, to the effective mass, m^*. The n^2 versus λ^2 plot shown in Fig. 7b is linear at higher wavelengths verifying Eq. (10). The values of ε_L and (N/m*) is determined by extrapolating the linear part to $\lambda^2=0$, from the slope and the intercept they were found to be 6, 4.498×10^{47} g^{-1} cm^{-3} for as-deposited and for irradiated film 3.69, 1.87×10^{47} g^{-1} cm^{-3} respectively. The disagreement between the values of the optical dielectric constant, ε_∞ and the lattice dielectric constant, ε_L, may be due to free-carrier contribution.

3.3. Energy gap determination

The optical band gap was determined from the analysis of the spectral dependence of the absorption near the fundamental absorption edges within the framework of one electron theory [24].

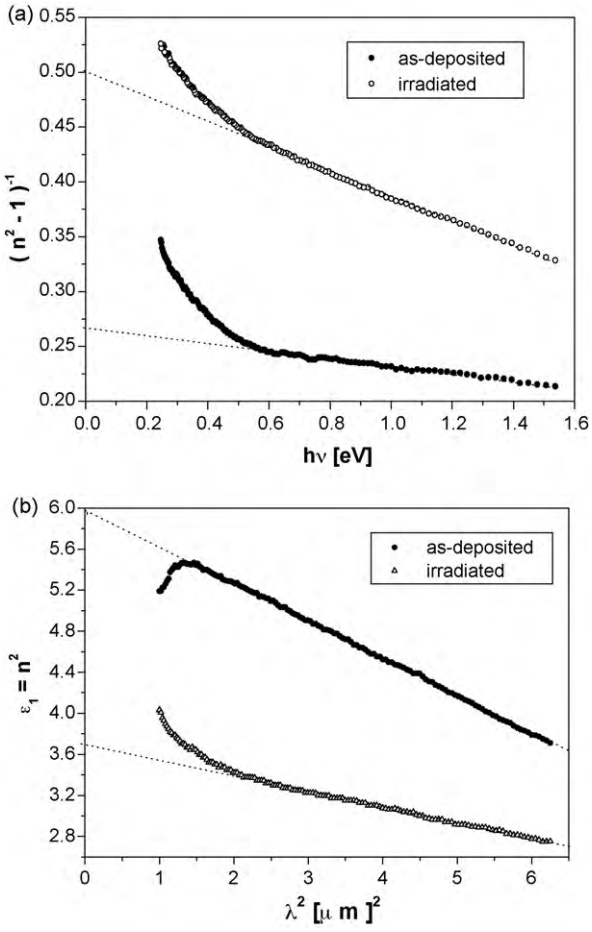

Fig. 7. (a) The plot of $(n^2-1)^{-1}$ against $(h\upsilon)^2$ for as-deposited and irradiated [(n-hexyl)$_8$PcRu] (**2**) thin films. (b) The plot of (n^2) against (λ^2) for as-deposited and irradiated [(n-hexyl)$_8$PcRu] (**2**) thin films.

This theory can be used to analyze the absorption edge data of molecular solids. The absorption coefficient α is well described by the relation [27]:

$$(\alpha h\upsilon)^{1/2} = G(h\upsilon - E_g^{ind}) \quad (11)$$

where E_g is the value of the optical band gap corresponding to transitions indicated, and the factor (G) depends on the transition probability which can be assumed to be constant within the optical frequency range. The $(\alpha h\upsilon)^{1/2}$ vs $(h\upsilon)$ plot for the as-deposited and the irradiated films is shown in Fig. 8. This is the characteristic behaviour of indirect transitions in non-crystalline materials. This type of transition is in well agreement with previous work [26,29,32]. The values for the corresponding energies were found to be 1.266, 1.57, 2 and 2.39 eV for the as deposited and 1.418, 2.33, and 3.2 eV for the irradiated films. It should be noted that the first energy value is the optical gap E_g^{opt}, corresponds to the onset of optical absorption and formation of a bound electron-hole pair, or exciton "Frenkel exciton" [33], but the last energy value is the fundamental energy gap (energy gap between valence band "π-band" and conduction band "π*-band" [34], and the values between them may be impurities energy levels.

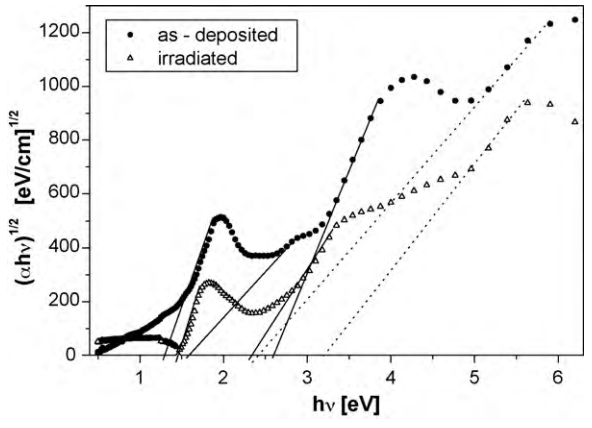

Fig. 8. The plot of $(\alpha h\upsilon)^{1/2}$ versus $(h\upsilon)$ for as-deposited and irradiated [(n-hexyl)$_8$PcRu] (**2**) thin films.

4. Conclusions

In this study, the XRD obtained for [(n-hexyl)$_8$PcRu] (**2**) powder confirms that the material is polycrystalline natural with triclinic structure and for thin films which confirmed the amorphous nature for as-deposited and irradiated films.

The optical properties of [(n-hexyl)$_8$PcRu] (**2**) before and after X-ray irradiations have been studied by means of spectrophotometric measurement in thin film form.

In the spectral range 200–2500 nm the refractive index showed anomalous dispersion in the wavelength range of (200–900 nm) while in the wavelength more than 900 nm, it is found that the refractive index dispersion data obeyed the single oscillator model. An interpretation of single oscillator parameters and Drude model of free carriers absorption have been described for the analysis of refractive index dispersion before and after irradiation. The amorphous nature of our samples is found to support the interpretation of indirect band gap.

References

[1] S.J. Yaghmour, J. Alloys Compd. 486 (2009) 284.
[2] M.M. El-Nahass, S. Yaghmour, Appl. Surf. Sci. 255 (2008) 1631.
[3] D. Klaus, R. Knecht, A. Dragässer, C. Keil, D. Schlettwein, Phys. Stat. Sol. A 206 (12) (2009) 2723.
[4] X. Tian, Z. Xu, F. Zhang, S. Zhao, G. Yuan, J. Li, Q. Sun, Y. Wang, Curr. Appl. Phys. 10 (2010) 129.
[5] K.-Y. Law, Chem. Rev. 93 (1993) 449.
[6] Y. Shirota, J. Mater. Chem. 10 (2000) 1.
[7] J.S. Huang, M. Pfeiffer, A. Werner, J. Blochwitz, K. Leo, S.Y. Liu, Appl. Phys. Lett. 80 (2002) 139.
[8] Z. Bao, A.J. Lovinger, J. Brown, J. Am. Chem. Soc. 120 (1998) 207.
[9] M. Ling, Z. Bao, Org. Electron. 7 (2006) 568.
[10] R. Caminiti, A. Capobianchi, P. Marovino, A.M. Poaletti, G. Padeletti, G. Pennesi, G. Rossi, Thin Solid Films 382 (2001) 74.
[11] M. Hanack, J. Osio-Barcina, E. Witke, J. Polymer Synth. 52 (1992) 211.
[12] M. Hanack, R. Polley, Synthesis 3 (1997) 295.
[13] T.E. Youssef, M. Hanack, J. Porphyrins Phthalocyanines 9 (1) (2005) 29.
[14] T.E. Youssef, Sean OïFlaherty, M. Werner Blau, Hanack, Eur. J. Org. Chem. 1 (2004) 101.
[15] T.E. Youssef, M. Hanack, J. Porphyrins & Phthalocyanines 6 (9 and 10) (2002) 573.
[16] A. Capobianchi, A.M. Paoletti, G. Pennesi, G. Rossi, R. Caminiti, C. Ercolani, Inorg. Chem. 33 (1994) 4635.
[17] L. Alagna, A. Capobianchi, M.P. Casaletto, G. Mattogno, A.M. Paoletti, G. Pennesi, G. Rossi, J. Mater. Chem. 11 (2001) 1928.
[18] M. Hanack, P. Haisch, H. Lehmann, L.R. Subramanian, Synthesis 4 (1993) 387.
[19] S. Tolansky, Multiple Beam Interferometry Surfaces and Films, Oxford, London, 1988, p. 147.
[20] M.M. El-Nahass, J. Mater. Sci. 27 (1992) 6592.
[21] A.M. Bakry, A.H. El-Naggar, Thin Solid Films 360 (2000) 293.
[22] Giulio, et al., Phys. Stat. Sol. A 136 (1993) K101.
[23] R. Shirley, The CRYSFIRE System for Automatic Powder Indexing: Use's Manual, The Lattice Press, England, 2000.
[24] J. Laugier, B. Bochu, LMGP-Suite of Programs for the Interpretation of X-ray Experiments, ENSP/Laboratories des Materiaux et du Genie Physique, BP46.38042, Saint Martin d'Heres, France, 2000.
[25] J.H. Sharp, M. Abkowitz, J. Phys. Chem. 77 (1973) 477.
[26] M.M. El-Nahass, A.A. Atta, H.E.A. El-Sayed, E.F.M. El-Zaidia, Appl. Surf. Sci. 254 (2008) 2460.
[27] M.M. El-Nahass, Z. El-Gohary, H.S. Soliman, Opt. Laser & Technol. 35 (2003) 523.

[28] M.M. El-Nahass, K.F. Abd-El-Rahman, A.A.A. Darwish, Mater. Chem. Phys. 92 (2005) 185.
[29] G.A. Kumar, J. Thomas, N. George, B.A. Kumar, P. Radhakrishnan, V.P.N. Poori, C.P.G. Vallabhan, N. Unnikrishnan, Phys. Chem. Glass 41 (2000) 89.
[30] H.S. Soliman, N. El-Kadry, O. Ganjoum, M.M. El-Nahass, H.B. Darwish, Indian J. Opt. 17 (64) (1988) 45.
[31] S.H. Wemple, M.D. DiDomenico Jr., Phys. Rev. B 3 (1970) 1338.
[32] R.A. Collins, A. Krie, A.K. Abass, Thin Solid Films 299 (1993) 113.
[33] E.V. Tsiper, Z.G. Soos, W. Gao, A. Kahn, Chem. Phys. Lett. 360 (2002) 47.
[34] U. Zhokhavets, R. Goldhahn, G. Gobsch, W. Schliefke, Synth. Met. 138 (2003) 491.